Proceedings of the ASME 2019
International Design Engineering Technical Conferences
and Computers and Information in Engineering Conference
IDETC/CIE2019
August 18-21, 2019, Anaheim, CA, USA

DETC2019-98056

KIRIGAMI-BASED DEPLOYABLE TRANSCREASE HARD STOP MODELS USABLE IN ORIGAMI PATTERNS

David W. Andrews
Compliant Mechanisms Research
Dept. of Mechanical Engineering
Brigham Young University
Provo, Utah 84602
Email: david.w.andrews@byu.net

Alex Avila
Compliant Mechanisms Research
Dept. of Mechanical Engineering
Brigham Young University
Provo, Utah 84602
Email: alexavila@byu.net

Jared Butler
Compliant Mechanisms Research
Dept. of Mechanical Engineering
Brigham Young University
Provo, Utah 84602
jaredbutler@byu.net

Spencer P. Magleby
Compliant Mechanisms Research
Dept. of Mechanical Engineering
Brigham Young University
Provo, Utah 84602
magleby@byu.edu

Larry L. Howell
Compliant Mechanisms Research
Dept. of Mechanical Engineering
Brigham Young University
Provo, Utah 84602
lhowell@byu.edu

ABSTRACT

Stopping origami in arbitrary fold states can present a challenge for origami-based design. In this paper two categories of kirigami-based models are presented for stopping the fold motion of individual creases using deployable hard stops. These models are transcrease (across a crease) and deploy from a flat sheet. The first category is planar and has behavior similar to a four-bar linkage. The second category is spherical and behaves like a degree-4 origami vertex. These models are based on the zero-thickness assumption of paper and can be applied to origami patterns made from thin materials, limiting the motion of the base origami pattern through self-interference within the original facets. Model parameters are based on a desired fold or dihedral angle, as well as facet dimensions. Examples show model benefits and limitations.

1 INTRODUCTION

Some origami-based applications call for the fold motion to stop at a predetermined state (e.g., for positioning optical components). The facet interference technique in partially folded states is a valuable blocking method for stopping motion in a desired fold state [1]. Facet interference cannot be implemented within an arbitrary pattern since it requires non-flat foldability. The dimensions and alignment of facets must be such that facets interfere in a desired fold angle [2]. Generally, patterns only allow for alterations to the fold pattern along the edges of the pattern. These changes can prove useful for single-degree of freedom patterns but become increasingly complex when a pattern has multiple degrees of freedom.

Kirigami is similar to origami, but includes both folding and cutting of paper. Cuts can be made to a preexisting origami pattern to change its original characteristics or develop entirely new patterns. Similar to kirigami are mechanisms commonly used in pop-up books, which also involve folding and cutting of pa-

per [3]. Recently, kirigami has found a number of applications, such as in the design of metamaterials [4].

This work presents four models, within two categories, for deployable hard stops within an origami pattern using kirigami. The models in the first category are similar to a pop-up book mechanism that deploys out of a plane. The models in the second category exhibit characteristics of a spherical linkage, employing a degree-4 vertex. Each hard stop model is developed across a crease and bounded by the facets adjacent to that crease, so as to reside within an origami pattern. Each model is defined, including equations for calculating hard stop model parameter values. Examples showing benefits and limitations of these models are also included.

2 BACKGROUND

This work adapts methods for blocking motion in origami and the art of kirigami to develop hard stop models for origami patterns. Additional background in the areas of motion blocking and kirigami is given below.

2.1 Blocking Motion

For origami patterns to stop moving in a desired configuration, a blocking mechanism must be introduced to reduce the patterns range of motion. Facet interference is a common technique for producing a hard stop to motion in a desired fold state [1] and utilizes self-interference of adjacent facets within an origami pattern [2]. Foschi and Tachi [2] outline a technique for determining which facet within a degree-4 origami vertex will block motion and how to design for a desired stop angle between facets. They also give an example of how their technique can be used in a multi-faceted origami pattern.

Establishing hard stops to motion becomes more challenging when an origami pattern has multiple degrees of freedom or does not allow adjacent facets to completely interfere. A mechanism built upon such a pattern cannot use facet interference to stop motion.

Ku [5] outlines a thickness based method for creating a hard stop in motion within an origami-based crease. This method requires removing material along one or both sides of the crease in such a way to allow motion along a given axis, but block motion at a desired angle. Thus, this method utilizes the thickness of the material being used. Many thick-folding techniques exhibit this behavior [6].

Shemenski and Trease [7] show an example of a deployable flasher with strings used as hard stops to stop motion in a partially folded state. They also show an example of a hard stop built into a hinge and discuss how it can be used between adjacent facets as both a joint and a hard stop.

2.2 Kirigami

As an adaptation on traditional origami, kirigami, the art of folding and cutting paper, has ridden in the wake of origami to gain similar notoriety. Kirigami shares many advantages of origami, such as planar manufacturing and scalability [8]. Kirigami has been used to create metamaterials [4], lattice structures for sandwich boards [9], and bandages with increased flexibility [10]. These and other existing kirigami techniques remove portions of material, rather than cutting slits. In contrast to current modeling practices for origami, the cuts in kirigami can provide motion that need not be modeled as a spherical mechanism.

Pop-up mechanism [3] or pop-up origami [11] are two terms used synonymously with kirigami. Pop-up mechanisms are widely used in creative mechanisms which deploy from sheets of paper. Like origami, these mechanisms can be modeled using kinematics to define their motion, allowing for analysis and definitions of similar deployable mechanisms [3].

3 PLANAR TRANSCREASE HARD STOP MODELS

A planar transcrease hard stop (PTHS) is a deployable hard stop that is formed across an origami crease. PTHSs are planar double-slit mechanisms [3] that can be modeled as a four-bar kinematic linkage. Rather than deploying from a fully folded state like a pop-up book mechanism, a PTHS deploys from an unfolded state. This section provides general and flat-foldable models for a PTHS and corresponding limitations. Since these models originate from a plane, they are equivalent to those of a change-point mechanism.

3.1 General Planar Transcrease Hard Stop

The general PTHS model can be realized by adding two slits through a crease between two adjacent facets, stretching between creases b and d, as shown in Figure 1. The initial crease and facets become the base of the PTHS model. The newly created facets, B and C, act as links with joints at creases b, c, and d. Folding the base facets, A and D, toward each other deploys the hard stop. At a desired angle, facet B interferes with facet A, blocking relative motion between facets A and D. This resulting hard stop to motion creates a partially folded fold state with a given dihedral angle, which is the angle between the normal vectors of adjacent facets [12].

Figure 2 shows the parameters for a general PTHS model, namely the dihedral angle (ρ_d) and model lengths (L_1, L_2, L_3, L_4). The general PTHS model may have an arbitrary shape or angle with respect to the base crease a, as long as creases b, c, and d remain parallel to a. The lengths are defined in the plane of motion, perpendicular to the creases. Such a mechanism is kinematically equivalent to this model. Three independent parameter values need to be selected to define the model. The two remaining parameter values are found using

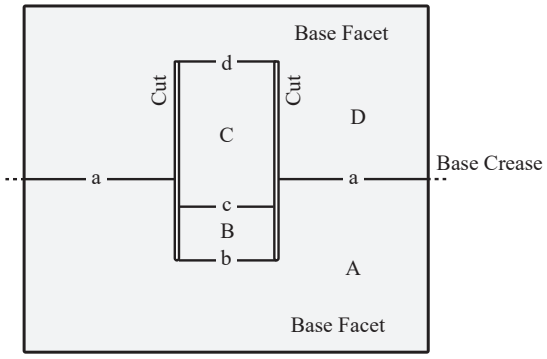

(a)

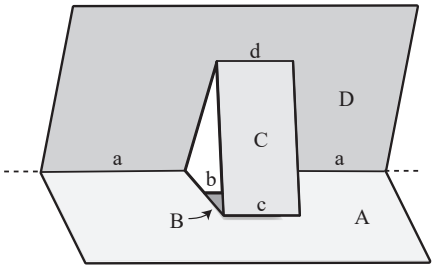

(b)

FIGURE 1. General PTHS model in (a) unfolded and (b) partially folded fold states. A and D are base facets. The base crease or gutter is denoted by *a*. B and C are the facets of the PTHS model.

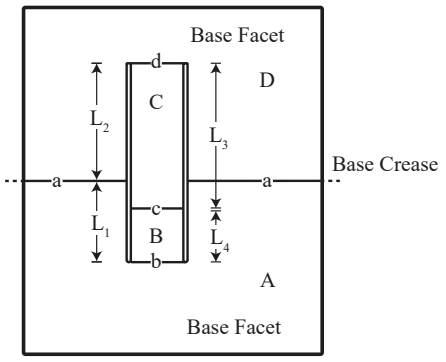

(a)

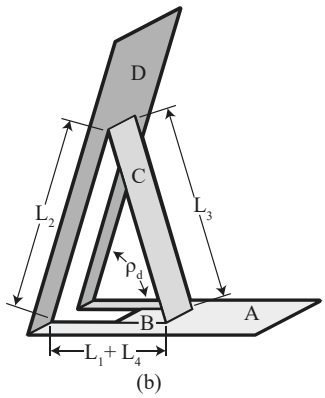

(b)

FIGURE 2. Parameters for a General PTHS model in (a) unfolded and (b) partially folded fold states.

$$L_1 + L_2 = L_3 + L_4 \tag{1}$$

and

$$L_3 = \frac{2L_1^2 + (2L_1L_2 + L_2^2)(1 - \cos\rho_d)}{2L_1 + L_2(1 - \cos\rho_d)} \tag{2}$$

which is derived using the law of cosines. The dihedral angle can be between 0° and 180°.

One advantage of the PTHS model is that it scales easily. Two non-dimensional ratios

$$R_{12} = \frac{L_1}{L_2} \tag{3}$$

and

$$R_{32} = \frac{L_3}{L_2} \tag{4}$$

can be used to define the PTHS model. The first, R_{12}, relates model lengths in the base facets (L_1, L_2). The second non-dimensional ratio, R_{32}, relates the angled links (L_2, L_3). As above, a value is first selected for ρ_d. Values for one length and one ratio are also selected. The remaining parameter values are found using equations (1), (3), (4) and

$$R_{32} = \frac{2R_{12}^2 + (2R_{12} + 1)(1 - \cos\rho_d)}{2R_{12} - \cos\rho_d + 1} \tag{5}$$

3.2 Flat-Foldable Planar Transcrease Hard Stop

A special case of the general PTHS model is the flat-foldable planar transcrease hard stop (FF-PTHS) model. For this model, shown in Figure 3, creases *a* and *c* are constrained to be coincident in the unfolded state. This constraint requires that $L_1 = L_4$ and $L_2 = L_3$, removing two model parameters. Further, this makes it possible for the FF-PTHS model to be deployed to create a partially folded state, while also being able to be flat-foldable, with creases *a* and *c* remaining coincident during motion. A trade-off of using this constraint is that it reduces the dihedral angle range to be 0° to 90°.

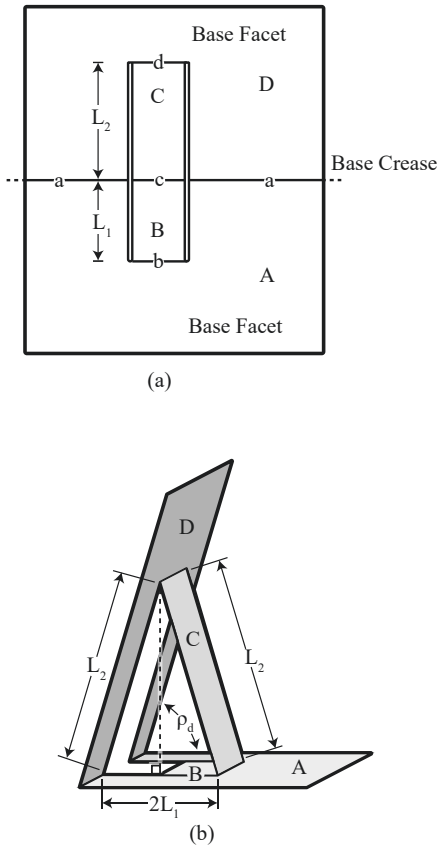

FIGURE 3. Parameters for a FF-PTHS model in (a) unfolded and (b) partially folded fold states.

Calculating the model parameter values is much simpler for this model than for the general PTHS model, because $R_{32} = 1$. This allows equation (5) to reduce to be

$$R_{12} = \cos\rho_d \quad (\text{for } R_{32} = 1) \tag{6}$$

This simplified model requires only two independent parameter values: ρ_d and either L_1 or L_2. The remaining length is found R_{12} given in equation (3).

3.3 Limitations

The parameters for both PTHS models are limited by the dihedral angle. For the general PTHS model, as ρ_d approaches 0°, L_3 and L_4 approach L_1 and L_2, respectively. Conversely, as ρ_d approaches 180°, L_3 reaches a limit of $L_1 + L_2$ and L_4 rapidly approaches a length of 0. This rapid approach causes the general PTHS model's efficiency to decrease quickly past 90°. For the FF-PTHS model, L_2 approaches infinite length as ρ_d approaches 90°. Additionally, both PTHS models are limited by the size of the base facets the hard stop model is formed from.

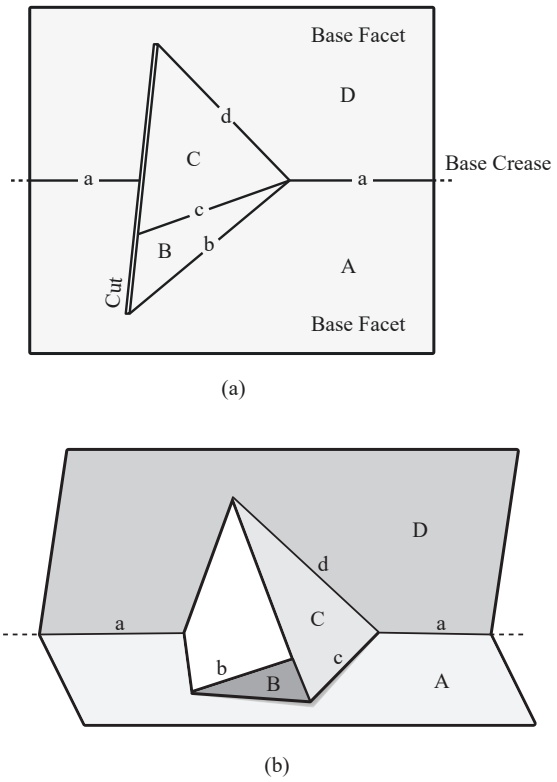

FIGURE 4. General STHS model in (a) unfolded and (b) partially folded fold states. A and D are base facets. The base crease or gutter is denoted by *a*. B and C are the facets of the STHS model.

4 SPHERICAL TRANSCREASE HARD STOP MODELS

A spherical transcrease hard stop (STHS) is a deployable hard stop that is formed across an origami crease. STHSs are single-slit spherical mechanisms [3] that act like a degree-4 origami vertex deploying from a plane. This section provides general and simplified models for a STHS and corresponding limitations.

4.1 General Spherical Transcrease Hard Stop

The general STHS model can be realized by adding a degree-4 origami vertex laying over a crease between two facets, as shown in Figure 4. A cut is made from tip to tip of creases *b* to *c* and *c* to *d*. Folding the base facets, A and D, toward each other deploys the hard stop. At a desired angle, facet B interferes with facet A, blocking relative motion between facets A and D. This resulting hard stop to motion creates a partially folded fold state with a given dihedral angle.

Figure 5 shows the parameters for a general STHS model , namely the dihedral angle (ρ_d) and vertex angles (θ_1, θ_2, θ_3, θ_4, θ_5). Like the general PTHS model, three independent parameter values need to be selected to define the model. The three remaining parameter values are found using

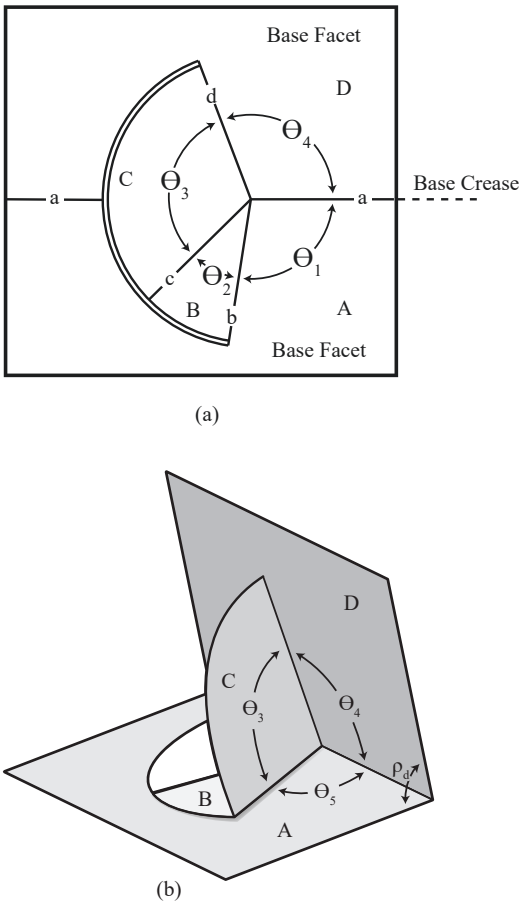

FIGURE 5. Parameters for a General STHS model in (a) unfolded and (b) partially folded fold states.

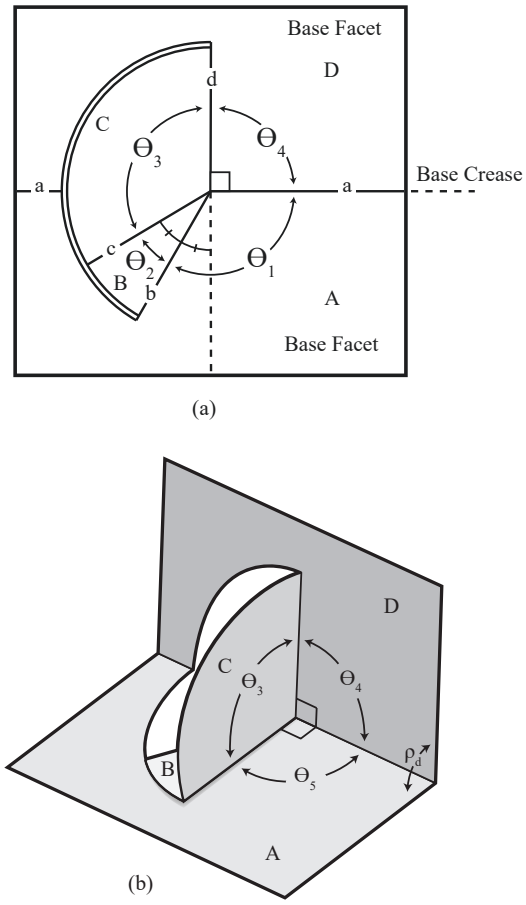

FIGURE 6. Parameters for a P-STHS model in (a) unfolded and (b) partially folded fold states.

$$\theta_1 + \theta_2 + \theta_3 + \theta_4 = 2\pi \tag{7}$$

$$\theta_5 = \theta_1 - \theta_2 \tag{8}$$

$$\cos\rho_d = \frac{\cos\theta_3 - \cos\theta_4\cos\theta_5}{\sin\theta_4\sin\theta_5} \tag{9}$$

with the last being derived from the spherical law of cosines.

For this model the dihedral angle can be between 0° and 180°. The shape of the kirigami facets is arbitrary, only being required to fit within the corresponding base facets. The figures in this paper show angled (Figure 4) and circular (Figures 5 and 6) examples.

By specifying an angle between facets A and C and between facets C and D, one has the necessary parameters for defining a spherical triangle originating from the center of the degree-4 vertex of the transcrease hard stop model. Using the spherical trigonometric laws of sines and cosines in conjunction with equations (7) through (9), one or both of the newly defined angles can be used as additional independent parameters to find model parameter values. These angles would replace vertex angles as independent parameters.

4.2 Perpendicular Spherical Transcrease Hard Stop

A special case of the general STHS model greatly simplifies the calculation of vertex angles by implementing specific constraints. This model is called the perpendicular spherical transcrease hard stop (P-STHS) model and the corresponding parameters are shown in Figure 6. The constraints for this model are that $\theta_4 = 90°$ and $\theta_5 = 90°$. These constraints lead to a simplified value of $\theta_3 = \rho_d$ as calculated by inserting the θ_4 and θ_5

constraint values into equation (9). These constraints cause the P-STHS model to always be perpendicular to the base facets.

To calculate the parameter values of the P-STHS model, only a single independent parameter value needs to be defined. This parameter is usually the dihedral angle, ρ_d. Equations (7) and (8) are used to find the last parameter values of θ_1 and θ_2.

4.3 Limitations

The most noticeable limitation of the general STHS model is that it is more complex than the general PTHS model. This is due to the complexities of spherical trigonometry. Much of this difficulty is removed for the P-STHS model by setting specific constraints.

As the dihedral angle approaches 0° or 180°, the hard stop approaches the limits of the model. At 0°,

$$\theta_1 + \theta_3 = \theta_2 + \theta_4 = \pi \tag{10}$$

which causes facets A and B to interfere and facets C and D to interfere, resulting in a fully folded degree-4 vertex. At 180°,

$$\theta_1 + \theta_4 = \theta_2 + \theta_3 = \pi \tag{11}$$

which causes the hard stop facets, B and C, to interfere with both facets A and D. This results in an unfolded state with a flap that is fully folded.

Like the PTHS models, the parameter values of STHS models are dependent on the size of the base facets the model is formed from. This is especially important near the model limits, where one or two vertex angles begin to rapidly decrease in size.

5 EXAMPLES

Two examples were created to show specific benefits of using this model. Corresponding limitations are also shown. Since these are models, prototypes were built using thin materials that require no adaptation for thickness. The first example shows how these models can be used to block motion within an origami pattern. The second example shows the range of possible dihedral angles from these models.

5.1 Motion Blocking Demonstration

The purpose of a hard stop is to block motion once a specific position or angle is reached. These transcrease hard stop models can be implemented directly into origami patterns because of the zero-thickness assumption of paper. For this example, we use a muira-ori pattern which has two flat states: fully unfolded and fully folded. Each hard stop in this model is based on the FF-PTHS model for its simplicity and for its dual deployable, fully-foldable nature.

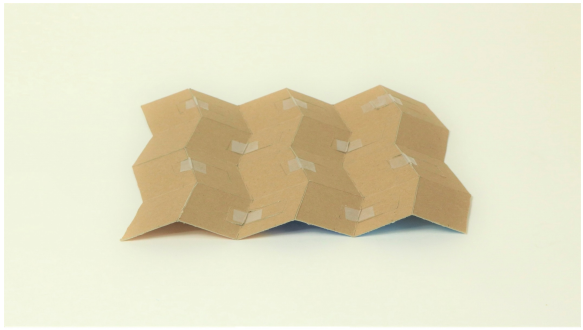

(a)

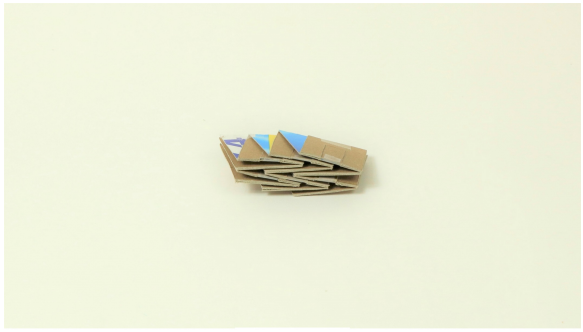

(b)

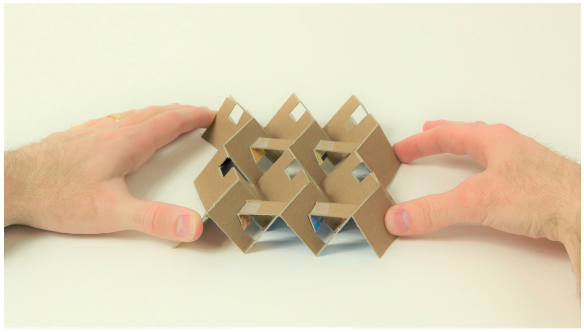

(c)

FIGURE 7. Muira-ori pattern containing transcrease hard stops based on the FF-PTHS model in (a) fully unfolded, (b) fully folded, and (c) partially folded/blocked states. The blocked state (c) is held in place under external loading.

As shown in Figure 7a, hard stops are placed in multiple adjacent facets directly across the crease, each having the same parameter values. The parameter values used were $rho_d = 60°$, $L_1 = 2$, and $L_2 = 4$. Figures 7a and b show the muira-ori pattern in its original folded states. Figure 7c shows each PTHS deployed, blocking the origami pattern from reaching its fully folded state. Each moves perpendicular to the crease it is across, yet is cut parallel to the other creases.

This example shows that these transcrease hard stop models can be used to develop hard stops that block motion within an origami pattern. Further, this example shows that the FF-PTHS model allows for 3 states as shown in the three portions of Figure 7. This is a specific benefit of the FF-PTHS model.

Since these are models and not fully realized design techniques, a complete stop to motion is not guaranteed. This can be seen in Figure 7c, where the flexibility of paper allows for the transcrease hard stops to bend before fully blocking motion. Further, this flexibility requires an external load to keep the transcrease hard stops held in the partially folded state.

5.2 Angle Range Demonstration

Brigham Young University's block 'Y' on the mountain east of campus has become a symbol of the university. The shape of the 'Y' has numerous different angles as shown in Figure 8a. We use this shape to show the range of angles for the transcrease hard stop models outlined. The P-STHS model was used because it is more efficient past 90° than the PTHS models and easier to calculate than the general STHS model.

The block 'Y' was constructed from a continuous strip of material. The material was split along the mirror line in Figure 8a, creating two separate open loops. These narrower strips were segmented with creases so the length of each facet is equal to the length of the corresponding line segment as shown in Figure 8. Depending on the available space, one or two hard stops were added to each crease using the P-STHS model. The dihedral angle, ρ_d, of each hard stop corresponds with the angle between the line segments. Figure 9 shows the physical prototype in open and closed positions.

This example shows the range of angles that can be realized using these transcrease hard stop models, included dihedral angles of 60°, 90°, 120°, and 150°. Additionally, this example demonstrates that the shape for the STHS model can be arbitrary. Straight cuts were selected for ease of prototyping. The circles at the center of each vertex depicted in Figure 8 were removed to accommodate the thickness of the material in the physical prototype.

6 DISCUSSION

Each deployable transcrease hard stop model is formed within two base facets, making shape flexible. Each model can be easily scaled. Since paper has approximately zero thickness, these models can be implemented directly in paper, such as in origami patterns. These models can be applied multiple times in a crease or in multiple creases of an origami pattern, as shown in the first example above.

The visual rendering of each category of models resemble a different type of structural support. The PTHS models look like a strut, that spans between the two base facets. The STHS models look like a rib, commonly used to reduce bending of thin angled walls. This models could be adapted to create methods for designing physical deployable transcrease hard stops that fulfill these structural purposes.

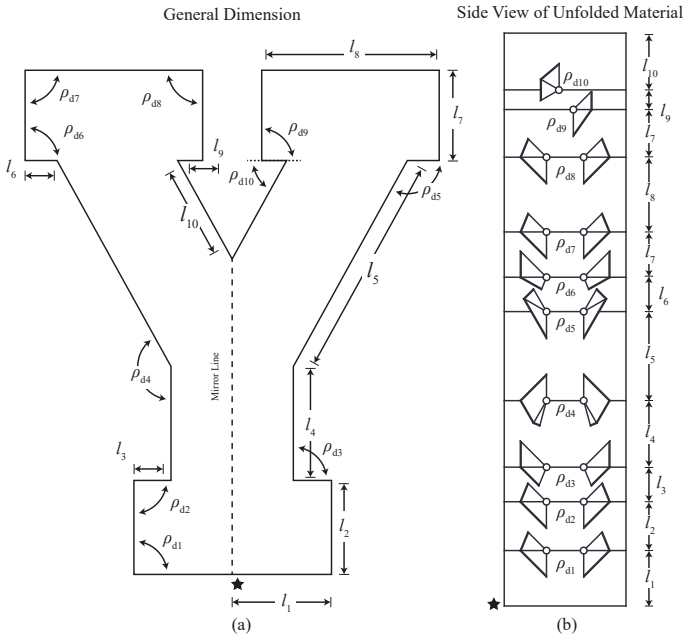

FIGURE 8. (a) The lengths and angles of the block Y. (b) One half of the block Y shown from the side with a mapping of the facet lengths and crease angles. All the creases have two P-STHSs to distribute the load, except for the top two creases which have insufficient space.

These deployable transcrease hard stop models are particularly valuable in origami patterns with multiple degrees of freedom. Using these models provides localized blocking within the pattern which can be fabricated simultaneously with the pattern itself, without adding additional material. The examples shown in Figure 7 and Figure 9 utilize this benefit.

The majority of model examples shown in this paper are perpendicular to the base crease. This does not need to be the case, as shown in Figure 4 and in the first example. Any hard stop orientation can be used as long as the conditions outlined for each model are satisfied.

7 CONCLUSION

This paper has presented four models for deployable transcrease hard stops, separated into two categories. For each category, a general and special case model were outlined. The models presented are theoretical, though they can be used directly in origami patterns, due to the near zero thickness attribute of paper. Examples are given in paper-like materials, which show specific benefits and limitations of these transcrease hard stop models.

FIGURE 9. BYU block Y designed using the P-STHS model in its open and closed positions. The shape is closed by pulling on a wire passing through each strip. The images are scaled to fit the page.

Future work will develop these models into methods and techniques that can be used for designing deployable transcrease hard stops for use in origami-based applications. This work will include mathematical adaptations of these models for thickness, strength and flexibility analysis, and discussion on designing to counteract motion challenges, such as singularities. This work also shows promise for extension to curved surfaces for use in developable mechanisms [13]. Additionally, work could be done to compare the suitability of methods developed from these models under static and dynamic loading.

ACKNOWLEDGMENT

This paper is based on work supported by the National Science Foundation and the Air Force Office of Scientific Research through NSF Grant No. EFRI-ODISSEI-1240417 and NSF Grant No. 1663345.

REFERENCES

[1] Avila, A., Magleby, S. P., Lang, R. J., et al., 2019. "Origami fold states: concept and design tool". *Mechanical Sciences,* ***10***(1), pp. 91–105.

[2] Foschi, R., and Tachi, T., 2018. "Designing self-blocking systems with non-flat-foldable degree-4 vertices". In Origami 7: The proceedings from the 7th international Meeting on Origami in Science, Mathmatics, and Education, Vol. 3, Tarquin, pp. 795–809.

[3] Winder, B. G., Magleby, S. P., and Howell, L. L., 2009. "Kinematic Representations of Pop-Up Paper Mechanisms". *Journal of Mechanisms and Robotics,* ***1***(2), p. 021009.

[4] Wang, F., Guo, X., Xu, J., Zhang, Y., and Chen, C. Q., 2017. "Patterning Curved Three-Dimensional Structures With Programmable Kirigami Designs". *Journal of Applied Mechanics,* ***84***(6), p. 061007.

[5] Ku, J. S., 2017. "Folding Thick Materials Using Axially Varying Volume Trimming". In Volume 5B: 41st Mechanisms and Robotics Conference, ASME, p. V05BT08A044.

[6] Lang, R. J., Tolman, K., Crampton, E., Magleby, S. P., and Howell, L. L., 2018. "Accommodating Thickness in Origami-Inspired Engineered Systems". *Applied Mechanics Reviews,* ***70***(January), pp. 1–20.

[7] Shemenski, P. D., and Trease, B. P., 2018. "Compact Directional and Frictional Hinges for Flat Folding Applications". In International Design Engineering Technical Conferences and Computers and Information in Engineering Conference, p. V05BT07A064.

[8] Blees, M. K., Barnard, A. W., Rose, P. A., Roberts, S. P., McGill, K. L., Huang, P. Y., Ruyack, A. R., Kevek, J. W., Kobrin, B., Muller, D. A., and McEuen, P. L., 2015. "Graphene kirigami". *Nature,* ***524***(7564), pp. 204–207.

[9] Li, Z., Chen, W., and Hao, H., 2018. "Crushing behaviours of folded kirigami structure with square dome shape". *International Journal of Impact Engineering,* ***115***(March 2017), pp. 94–105.

[10] Hwang, D. G., Trent, K., and Bartlett, M. D., 2018. "Kirigami-Inspired Structures for Smart Adhesion". *ACS Applied Materials and Interfaces,* ***10***(7), pp. 6747–6754.

[11] Bernard, A., Aguiar, C. D., Green, K. E., and Member, S., 2018. "Model for a Rigid, 3D Mechanism Inspired by Pop-Up Origami, and its Application to a Reconfigurable, Physical Environment". *2018 IEEE 14th In-*

ternational Conference on Automation Science and Engineering (CASE), pp. 1146–1151.

[12] Lang, R. J., 2018. *Twists, Tilings and Tessellations. Mathematical methods for Geometric Origami.* A K Peters/CRC Press.

[13] Nelson, T. G., Zimmerman, T. K., Magleby, S. P., Lang, R. J., and Howell, L. L., 2019. "Developable mechanisms on developable surfaces". *Science Robotics,* ***5171***(February).